Alexandria Engineering Journal (2014) 53, 929–937

HOSTED BY

Alexandria University

Alexandria Engineering Journal

www.elsevier.com/locate/aej
www.sciencedirect.com

ORIGINAL ARTICLE

Unsteady MHD boundary-layer flow and heat transfer of nanofluid over a permeable shrinking sheet in the presence of thermal radiation

Samir Kumar Nandy [a,*], Sumanta Sidui [b], Tapas Ray Mahapatra [c]

[a] Department of Mathematics, A.K.P.C Mahavidyalaya, Bengai, Hooghly 712 611, India
[b] Department of Mathematics, Ajhapur High School, Ajhapur, Burdwan 713 401, India
[c] Department of Mathematics, Visva-Bharati, Santiniketan 731 235, India

Received 3 July 2014; revised 3 September 2014; accepted 7 September 2014
Available online 7 October 2014

KEYWORDS

Unsteady flow;
Heat transfer;
Magnetic field;
Thermal radiation;
Shrinking sheet

Abstract Forced convection in unsteady boundary layer flow of nanofluid over a permeable shrinking sheet in the presence of thermal radiation is studied. A variable magnetic field is applied normal to the sheet. The nanofluid model includes Brownian motion and thermophoresis effects. The governing momentum, energy and nanofluid solid volume fraction equations are solved numerically using fourth order Runge–Kutta method with shooting technique. The effects of various physical parameters on dimensionless velocity, temperature, nanoparticle volume fraction, as well as the skin friction, local Nusselt and local Sherwood numbers are analyzed. The numerical results indicate that dual solutions exist for certain values of the magnetic parameter (M), wall mass suction (s) and unsteadiness parameter (A). It is found that both magnetic field and wall mass suction widen the range of unsteadiness parameter for which the solution exists. The skin friction coefficient, local Nusselt and Sherwood numbers increase for the first solution and decrease for the second solution with the increase in M.

1. Introduction

The boundary layer flow of an electrically conducting fluid in the presence of magnetic field has wide applications in many engineering problems such as MHD generator, plasma studies, nuclear reactors, geothermal energy extraction, and oil exploration. Also, radiative heat transfer in the boundary layer flow is very important from application point of view, because the quality of the final product is very much dependent on the rate of heat transfer of the ambient fluid particles. Again unsteady flows, such as start-up process and periodic fluid motion, are very much important in engineering practices. In many engineering problems, such as helicopter rotor, the ship propeller, the cascades of blades of turbo-machinery unsteady environment occurs. Hence it is very much important to

* Corresponding author. Tel.: +91 9434667221; fax: +91 3211 246772.
E-mail address: nandysamir@yahoo.com (S.K. Nandy).
Peer review under responsibility of Faculty of Engineering, Alexandria University.

http://dx.doi.org/10.1016/j.aej.2014.09.001

Nomenclature

A	nondimensional unsteadiness parameter
B	variable magnetic field
B_0	uniform magnetic field
c	constant proportional to the shrinking velocity
c_f	skin friction coefficient
c_p	specific heat at constant pressure
C	nanoparticle volume fraction
C_w	nanoparticle volume fraction at the surface
C_∞	nanoparticle volume fraction in the free stream
D_B	Brownian diffusion coefficient
D_T	thermophoresis diffusion coefficient
$f(\eta)$	dimensionless stream function
K_1	mean absorption coefficient
Le	Lewis number
M	dimensionless magnetic parameter
Nb	dimensionless Brownian motion parameter
Nt	dimensionless Thermophhoresis motion parameter
Nu_x	local Nusselt number
Pr	Prandtl number
Pr_{eff}	effective Prandtl number
q_m	wall mass flux
q_w	wall heat flux
R	thermal radiation parameter
Re_x	local Reynolds number
s	mass suction parameter
Sh_x	local Sherwood number
T	temperature of the fluid
T_w	temperature of the fluid at the sheet
T_∞	temperature of the fluid in the free stream
u, v	velocity components along x and y axes, respectively
u_w	velocity of the shrinking sheet
v_w	velocity of mass transfer

Greek symbols

α_m	thermal diffusivity
$\phi(\eta)$	rescaled nanoparticle volume fraction
η	similarity variable
θ	dimensionless temperature of the fluid
ν	kinematic viscosity of the fluid
λ	dimensional unsteadiness parameter
ρ_f	density of the base fluid
τ	ratio of the effective heat capacity of the nanoparticle material and the ordinary fluid
ψ	stream function

investigate the simultaneous effects of thermal radiation, magnetic field and unsteadiness.

Various industries such as chemical production, power generation in a power plant, production of microelectronics, advanced nuclear systems demand an efficient heat exchanger device. Classical heat transfer fluids such as water, ethylene glycol, engine oil have a limitation in heat transfer efficiency. In contrast, metals are very good conductors. To overcome this disadvantage of fluids, it would be desired to combine metals and fluids to produce a heat transfer medium that behaves like a fluid, but has the thermal conductivity of a metal. The necessity for improving the thermal conductivity and enhancing the heat transfer has led to the utilization of nanoparticles in the fluid.

A liquid containing suspension of a metallic (such as Cu, Al, Fe, Hg and Ti) or a non-metallic (such as metal oxide) nanometer-sized (generally less than 100 nm) solid particles or fibers is termed as nanofluid. The main characteristics of the nanofluid are the enhancement of the thermal conductivity of the base fluid, minimal clogging in few passage, long term stability and homogeneity (see Choi [1], Choi et al. [2]). Because of the wide range of applications of nanofluids, significant research has been carried out in recent years by the researchers to study the heat transfer characteristics of these fluids.

Buongiorno [3] was the first who formulated the nanofluid model taking into account the effects of Brownian motion and thermophoresis. In his work, he has pointed that although there are some elements those affect nanofluid flow such as inertia, Brownian diffusion, thermophoresis, Magnus effect, fluid drainage, diffusiophoresis and gravity; only Brownian diffusion and thermophoresis are important mechanisms in nanofluid. It should be mentioned that a lot of researchers (see [4–6]) have used the mathematical nanofluid model proposed by Buongiorno [3] to study different problems under different physical situations.

Bachok et al. [7] investigated the forced convective boundary layer flow of nanofluid over a moving plate and they concluded that dual solutions exist when the plate and free stream move in opposite directions. Khan and Pop [8] analyzed the boundary layer flow and heat transfer of nanofluid over a stretching surface. The effect of magnetic field on free convection flow of nanofluid past a vertical flat plate was considered by Hamad [9]. The boundary layer flow and heat transfer in a viscous fluid containing metallic nanoparticles over a nonlinear stretching sheet are investigated by Hamad and Ferdows [10]. They studied different types of nanoparticles and found that the behavior of the fluid flow changes with the change of type of the nanoparticles. Numerous recent studies on nanofluids can be found in [11–15].

Recently, the boundary layer flow near a shrinking sheet gets attention due to increasing engineering applications. The existence and uniqueness of steady viscous flow due to a shrinking sheet was established by Miklavcic and Wang [16] and they concluded that for some specific value of suction at the sheet, dual solutions exist and also in certain range of value of suction, no boundary layer solution exists. On the other hand, Wang [17] investigated the stagnation point flow toward a shrinking sheet and obtained dual solutions for some values of the ratio of shrinking and stagnation flow rates. Following these works, some very important investigations in this direction were made (see [18–23]).

The problem of boundary layer flow over a shrinking sheet with mass transfer is investigated by Fang et al. [24]. In that paper, they reported that boundary layer solution exists only for mass suction parameter $s \geqslant 2$ and for the unsteadiness

parameter $\beta \leqslant 0$. Later, Bachok et al. [25] analyzed the unsteady three dimensional boundary layer flow due to a permeable shrinking sheet. In another paper, Bachok et al. [26] studied the unsteady boundary layer flow and heat transfer of a nanofluid over a permeable stretching/shrinking sheet and they concluded that the unsteadiness parameter as well as the mass suction parameter widen the range of stretching/shrinking parameter for which the boundary layer solution exists. Very recently, the unsteady flow and heat transfer over an unsteady shrinking sheet with suction in a nanofluid was analyzed by Rohni et al. [27] and it was found that dual solutions exist for a certain range of wall mass suction, unsteadiness and nanofluid parameters.

The aim of the present paper (which is an extension of Rohni et al. [27]) is to study the simultaneous effect of the magnetic field and thermal radiation on the flow and heat transfer due to the unsteady, two-dimensional laminar flow of a viscous nanofluid caused by a permeable shrinking sheet. In this paper, a similarity analysis is performed to reduce the governing equations to ordinary differential equations which are subsequently solved numerically using fourth order Runga–Kutta method with shooting technique. Results presented focus on how the magnetic field, surface mass transfer, Brownian motion, thermophoresis and thermal radiation affect the heat and mass transfer characteristics of the flow. The present study is of immediate interest to all those which are highly affected with heat enhancement concept.

2. Flow analysis

Consider unsteady two-dimensional laminar boundary-layer flow of incompressible electrically conducting viscous nanofluid past a permeable shrinking sheet. The flow is subjected to a transverse magnetic field of strength B which is assumed to be applied in the positive y-direction, normal to the surface. It is assumed that the velocity of the shrinking sheet is $u_w(x,t)$ and the velocity of the mass transfer is $v_w(x,t)$, where x is the coordinate measured along the shrinking sheet and t is the time. It is also assumed that the constant surface temperature and concentration of the sheet are T_w and C_w, while the uniform temperature and concentration far from the sheet are T_∞ and C_∞, respectively.

Under these assumptions, the unsteady boundary-layer equations governing the flow, heat and mass transfer are

$$\frac{\partial u}{\partial x}+\frac{\partial v}{\partial y}=0 \tag{1}$$

$$\frac{\partial u}{\partial t}+u\frac{\partial u}{\partial x}+v\frac{\partial u}{\partial y}=\nu\frac{\partial^2 u}{\partial y^2}-\frac{\sigma B^2}{\rho_f}u \tag{2}$$

$$\frac{\partial T}{\partial t}+u\frac{\partial T}{\partial x}+v\frac{\partial T}{\partial y}=\alpha_m\frac{\partial^2 T}{\partial y^2}-\frac{1}{\rho_f c_p}\frac{\partial q_r}{\partial y}+\tau\left[D_B\frac{\partial C}{\partial y}\frac{\partial T}{\partial y}+\frac{D_T}{T_\infty}\left(\frac{\partial T}{\partial y}\right)^2\right] \tag{3}$$

$$\frac{\partial C}{\partial t}+u\frac{\partial C}{\partial x}+v\frac{\partial C}{\partial y}=D_B\frac{\partial^2 C}{\partial y^2}+\frac{D_T}{T_\infty}\frac{\partial^2 T}{\partial y^2}, \tag{4}$$

where u and v are the velocity components in the x and y-directions respectively, ν is the kinematic viscosity, σ is the electrical conductivity (assumed constant), ρ_f is the density of the base fluid, α_m is the thermal diffusivity, D_B is the Brownian diffusion coefficient, D_T is the thermophoresis diffusion coefficient and c_p is the specific heat at constant pressure. Here τ is the ratio of the effective heat capacity of the nanoparticle material and the heat capacity of the ordinary fluid, T is the fluid temperature and C is the nanoparticle volume fraction.

The term $\frac{\sigma B^2}{\rho_f}u$ in the R.H.S. of Eq. (2) is the Lorentz force which arises due to the interaction of the fluid velocity and the applied magnetic field. In writing Eq. (2), we have neglected the induced magnetic field since the magnetic Reynolds number for the flow is assumed to be very small. This assumption is justified for flow of electrically conductive fluids such as liquid metals e.g. mercury, liquid sodium, etc. (see Shercliff [28]). Eq. (3) depicts that heat can be transported in a nanofluid by convection, by conduction and also by virtue of nanoparticle diffusion and radiation. The term $u\frac{\partial T}{\partial x}+v\frac{\partial T}{\partial y}$ is the heat convection, the term $\alpha_m\frac{\partial^2 T}{\partial y^2}$ is the heat conduction; the term $\tau D_B\frac{\partial C}{\partial y}\frac{\partial T}{\partial y}$ is the thermal energy transport due to Brownian diffusion, the term $\tau\frac{D_T}{T_\infty}\left(\frac{\partial T}{\partial y}\right)^2$ is the energy transport due to thermophoretic effect and $\frac{1}{\rho_f c_p}\frac{\partial q_r}{\partial y}$ is the nanoparticle heat diffusion by radiation. Eq. (4) shows that the nanoparticles can move homogeneously within the fluid (by the term $u\frac{\partial C}{\partial x}+v\frac{\partial C}{\partial y}$), but they also possess a slip velocity relative to the fluid due to Brownian diffusion $D_B\frac{\partial^2 C}{\partial y^2}$ and the thermophoresis $\frac{D_T}{T_\infty}\frac{\partial^2 T}{\partial y^2}$.

Here the boundary conditions are

$$u=u_w(x,t)=-\frac{cx}{1-\lambda t}, v=v_w(x,t), T=T_w, \quad C=C_w \text{ at } y=0,$$
$$u\to 0, \quad T\to T_\infty, \quad C\to C_\infty \text{ as } y\to\infty, \tag{5}$$

The wall mass transfer velocity then becomes

$$v_w(x,t)=-\sqrt{\frac{c\nu}{1-\lambda t}}s, \tag{6}$$

where s is the constant wall mass transfer parameter with $s>0$ for suction and $s<0$ for injection, respectively. Using Rosseland's approximation for radiation (see Brewster [29]), we can write

$$q_r=-\frac{4\sigma_1}{3K_1}\frac{\partial T^4}{\partial y}, \tag{7}$$

where σ_1 is the Stefan–Boltzmann constant and K_1 is the mean absorption coefficient. Assuming the temperature difference within the flow is such that T^4 may be expanded in a Taylor series about T_∞ and neglecting higher order terms we get $T^4\approx 4T_\infty^3 T-3T_\infty^4$. Hence from Eq. (7), using the above result, we have

$$\frac{\partial q_r}{\partial y}=-\frac{16\sigma_1 T_\infty^3}{3K_1}\frac{\partial^2 T}{\partial y^2}, \tag{8}$$

To attain the similarity solutions of the Eqs. (1)–(4) with the boundary conditions (5), we take the transverse unsteady magnetic field strength applied to the sheet is of the form $B=B_0/\sqrt{1-\lambda t}$, where B_0 is constant. This form of $B_0(t)$ has also been considered by Vajravelu et al. [30] while analyzing the MHD flow and heat transfer over an unsteady stretching sheet. The stream function and dimensionless variable can be taken as

$$\psi = \sqrt{\frac{cv}{1-\lambda t}} x f(\eta), \quad \theta(\eta) = \frac{T - T_\infty}{T_w - T_\infty},$$
$$\phi(\eta) = \frac{C - C_\infty}{C_w - C_\infty}, \quad \eta = y\sqrt{\frac{c}{v(1-\lambda t)}}, \tag{9}$$

where the stream function ψ is defined in the usual way $u = \partial\psi/\partial y$ and $v = -\partial\psi/\partial x$. Substituting (9) into Eqs. (1)–(4), we obtain the following ordinary differential equations

$$f''' + ff'' - f'^2 - A\left(f' + \frac{\eta}{2}f''\right) - Mf' = 0, \tag{10}$$

$$\frac{1}{Pr_{eff}}\theta'' + f\theta' - A\frac{\eta}{2}\theta' + Nb\theta'\phi' + Nt\theta'^2 = 0, \tag{11}$$

$$\phi'' + Le\left(f - A\frac{\eta}{2}\right)\phi' + \frac{Nt}{Nb}\theta'' = 0, \tag{12}$$

where

$$M = \frac{\sigma B_0^2}{\rho_f c}, \quad A = \frac{\lambda}{c}, \quad Pr_{eff} = \frac{Pr}{1+4R/3}, \quad R = \frac{4\sigma_1 T_\infty^3}{K_1 \alpha_m \rho_f c_p}, \quad Pr = \frac{v}{\alpha_m},$$
$$v = \frac{\mu}{\rho_f}, \quad Nb = \frac{\tau D_B (C_w - C_\infty)}{v}, \quad Nt = \frac{\tau D_T (T_w - T_\infty)}{vT_\infty}, \quad Le = \frac{v}{D_B}. \tag{13}$$

Here M is the dimensionless magnetic parameter, A is the unsteadiness parameter, Pr_{eff} is the effective Prandtl number, R is the thermal radiation parameter, Pr is the Prandtl number, v is the kinematic viscosity of the fluid, Nb is the Brownian motion parameter, Nt is the thermophoresis parameter and Le is the Lewis number.

It is worth noting that the temperature actually does not depend on Prandtl number (Pr) and the thermal radiation parameter (R) independently, but depends only on a combination of them termed as effective Prandtl number Pr_{eff} which is directly proportional to the Prandtl number and inversely proportional to the thermal radiation parameter.

The corresponding boundary conditions are

$$f(0) = s, \; f'(0) = -1, \; \theta(0) = 1, \; \phi(0) = 1$$
$$f'(\infty) = 0, \quad \theta(\infty) = 0, \quad \phi(\infty) = 0. \tag{14}$$

The physical quantities of interest are the skin friction coefficient C_f, the local Nusselt number Nu_x and the local Sherwood number Sh_x which are defined as

$$C_f = \frac{\tau_w}{\rho_f u_w^2}, \qquad Nu_x = \frac{xq_w}{k(T_w - T_\infty)}, Sh_x = \frac{xq_m}{D_B(C_w - C_\infty)}, \tag{15}$$

where τ_w is the shear stress at the stretching surface, q_w and q_m are the wall heat and mass fluxes, respectively.

Hence using Eq. (10) we get

$$Re_x^{1/2} C_f = f''(0), \quad Nu_x Re_x^{-1/2} = -\theta'(0), \quad Sh_x Re_x^{-1/2} = -\phi'(0) \tag{16}$$

where $Re_x = u_w(x,t)x/v$ is the local Reynolds number based on the stretching velocity $u_w(x,t)$.

3. Numerical solution

By using a similarity transformation, the governing equations of the problem are reduced to a system of coupled, non-linear ordinary differential equations, which are solved numerically by fourth order Runga–Kutta method with shooting technique (see for details Gladwell and Sayers [31]). For the sake of brevity, further details of the solution process are not presented here. Since the physical domain in this problem is unbounded, whereas the computational domain has to be finite, we apply the far field boundary conditions for the similarity variable η at a finite value denoted by η_{max}. In all our computations we have used the value of $\eta_{max} = 12$ which is sufficient to satisfy the far field boundary conditions asymptotically for all values of the physical parameters considered in this problem. For these numerical computations, a uniform step size $\Delta\eta = 0.01$ is taken and the solutions are obtained with an absolute error tolerance of 10^{-6} in all cases.

4. Results and discussion

The analysis of the results obtained by the applied numerical scheme explores the condition for which the boundary layer solutions are possible. Following Fang et al. [24] and Rohni et al. [27], we have considered the decelerating shrinking sheet only (i.e., $A \leqslant 0$). To assess the accuracy of the present results, comparison of the critical values of A (i.e A_c, beyond which the boundary layer solution is not possible) between the present results and the previously published results are made for special cases (in the absence of magnetic field and thermal radiation) and found excellent agreement. This gives us confidence of our numerical results (see Table 1).

Numerical computations are carried out for several sets of values of the governing parameters, namely, unsteadiness parameter (A), magnetic parameter (M), thermal radiation parameter (R), effective Prandtl number (Pr_{eff}), Brownian motion parameter (Nb), thermophoresis parameter (Nt), Lewis number (Le) and suction parameter (s) using the numerical procedure discussed in the previous section. In order to illustrate the salient features of the model, the numerical results are presented in Figs. 1–15.

Fig. 1 shows that the dual solutions of skin friction coefficient $f''(0)$ with the unsteadiness parameter $A(<0)$ for several values of the magnetic parameter M. It reveals that it is possible to get dual solutions of the boundary layer equations for $A < 0$. These dual solutions are in the range $A_c \leqslant A < 0$ and no solution exists for $A < A_c < 0$, where A_c is the minimum value of A for which the solution exists. The value of A_c for different values of M are shown in figure. It is observed that the value of $|A_c|$ increases as the strength of the magnetic parameter increases. This shows that as the value of M increases the range of the values of A for which the solution of the boundary layer equations exists, also increases. Also, for a certain mass suction parameter ($s = 2.1$), in the case of upper solution branch, $f''(0)$ increases with the increase of M. However, for the lower solution branch, opposite trend is observed. The variation of $f''(0)$ with $A(<0)$ for different values of mass suction parameter s are depicted in Fig. 2. The fig-

Table 1 Comparison of the critical values of unsteadiness parameter A_c for several values of suction parameter s with $M = 0$.

s	Present study	Rohni et al. [27]
2.10	−1.654850	−1.6550
2.15	−3.860346	−3.8605
2.20	−8.349103	−8.3488

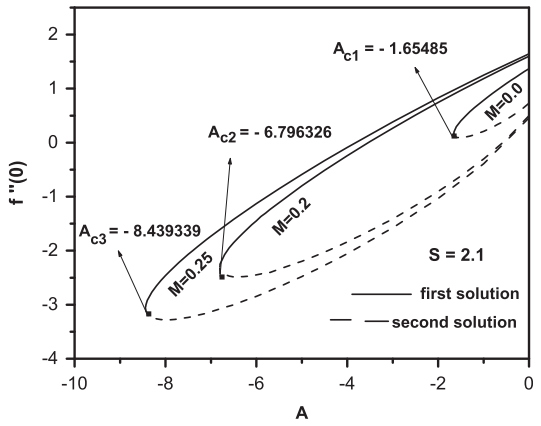

Figure 1 Dual solutions of skin friction coefficient $f''(0)$ with $A(<0)$ for several values of M when $s = 2.1$.

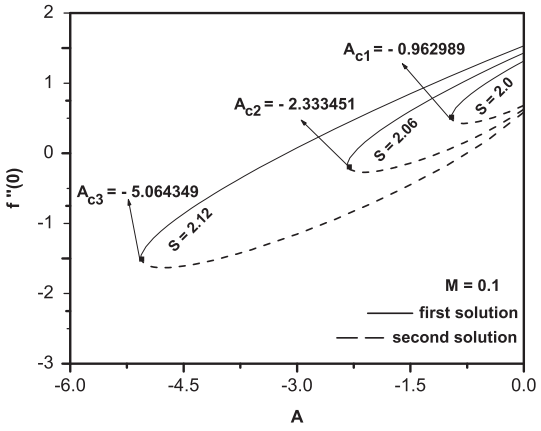

Figure 2 Dual solutions of skin friction coefficient $f''(0)$ with $A(<0)$ for several values of s when $M = 0.1$.

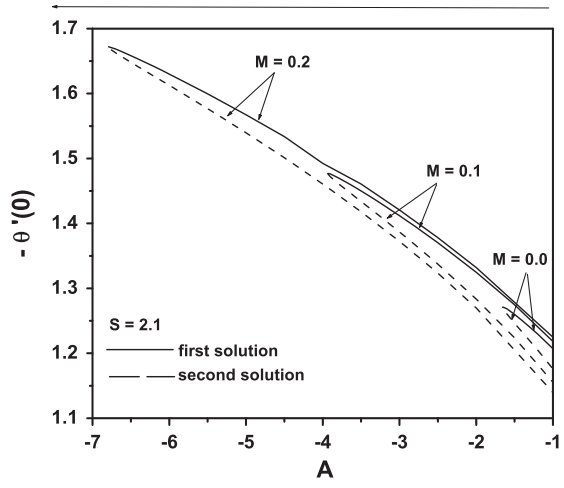

Figure 3 Variation of $-\theta'(0)$ with A for several values of M when $s = 2.1,\ Le = 2.0,\ Nb = 0.5,\ Nt = 0.5$ and $Pr_{eff} = 1.0$.

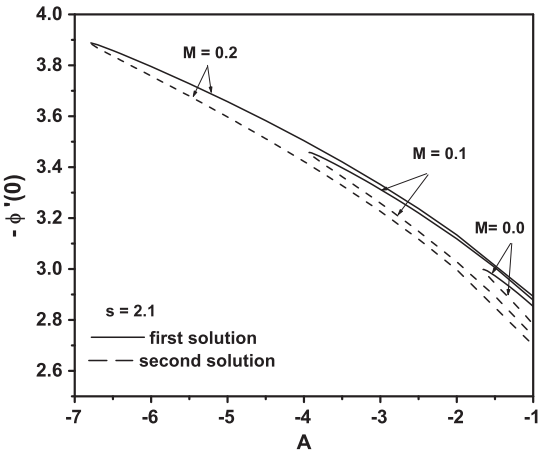

Figure 4 Variation of $-\phi'(0)$ with A for several values of M when $s = 2.1,\ Le = 2.0,\ Nb = 0.5,\ Nt = 0.5$ and $Pr_{eff} = 1.0$.

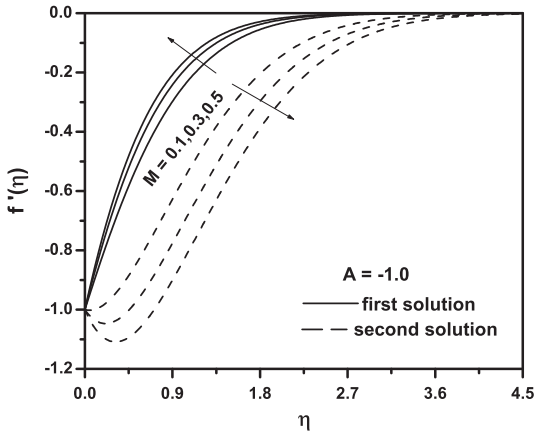

Figure 5 Variation of $f'(\eta)$ for several values of M when $s = 2.1$, $A = -1.0,\ Le = 2.0,\ Nb = 0.5,\ Nt = 0.5$ and $Pr_{eff} = 0.71$.

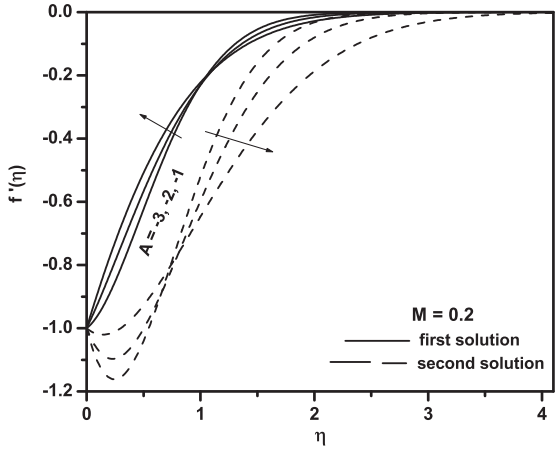

Figure 6 Variation of $f'(\eta)$ for several values of A when $s = 2.1$, $M = 0.2,\ Le = 2.0,\ Nb = 0.5,\ Nt = 0.5$ and $Pr_{eff} = 0.71$.

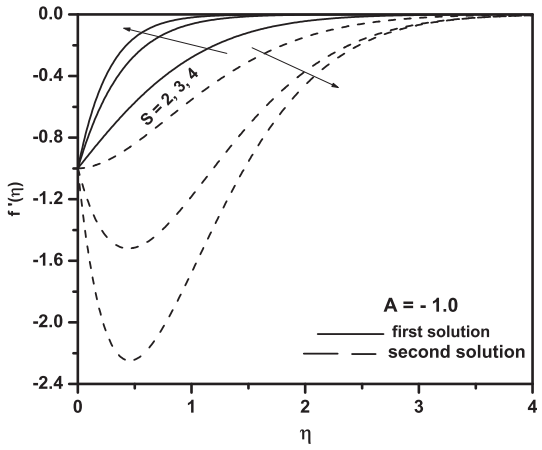

Figure 7 Variation of $f'(\eta)$ for several values of s when $A = -1.0$, $M = 0.2$, $Le = 2.0$, $Nb = 0.5$, $Nt = 0.5$ and $Pr_{eff} = 0.71$.

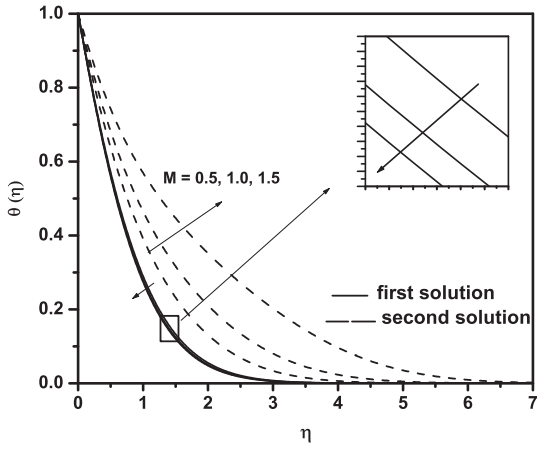

Figure 8 Variation of $\theta(\eta)$ for several values of M when $s = 2.0$, $A = -1.0$, $Le = 2.0$, $Nb = 0.5$, $Nt = 0.5$ and $Pr_{eff} = 0.71$.

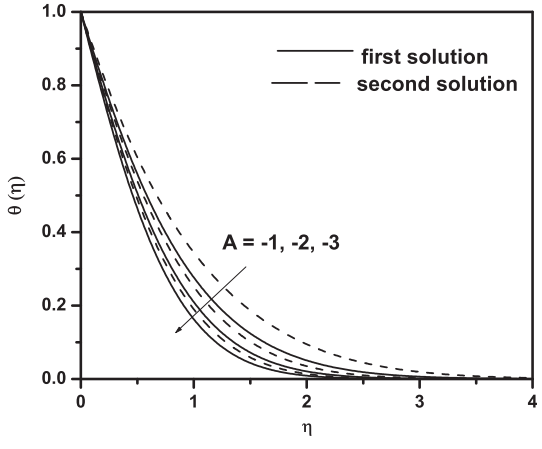

Figure 9 Variation of $\theta(\eta)$ for several values of A when $s = 2.1$, $M = 0.2$, $Le = 2.0$, $Nb = 0.5$, $Nt = 0.5$ and $Pr_{eff} = 0.71$.

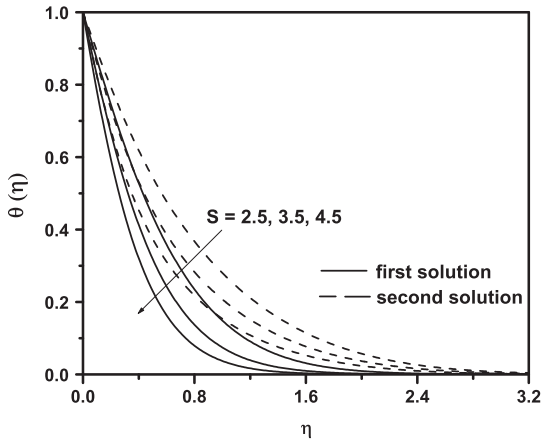

Figure 10 Variation of $\theta(\eta)$ for several values of s when $M = 1.0$, $A = -2.0$, $Le = 2.0$, $Nb = 0.5$, $Nt = 0.5$ and $Pr_{eff} = 0.71$.

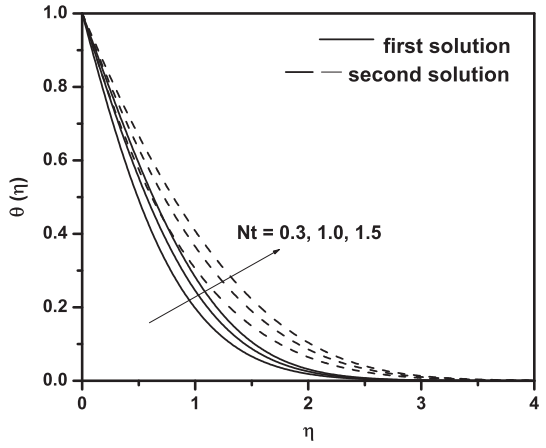

Figure 11 Variation of $\theta(\eta)$ for several values of Nt when $s = 2.0$, $M = 1.0$, $A = -2.0$, $Le = 2.0$, $Nb = 0.5$, and $Pr_{eff} = 0.71$.

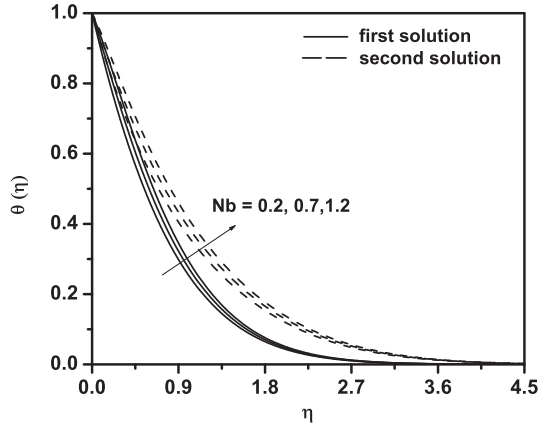

Figure 12 Variation of $\theta(\eta)$ for several values of Nb when $s = 2.1$, $A = -1.0$, $M = 0.5$, $Le = 2.0$, $Nt = 0.5$ and $Pr_{eff} = 0.71$.

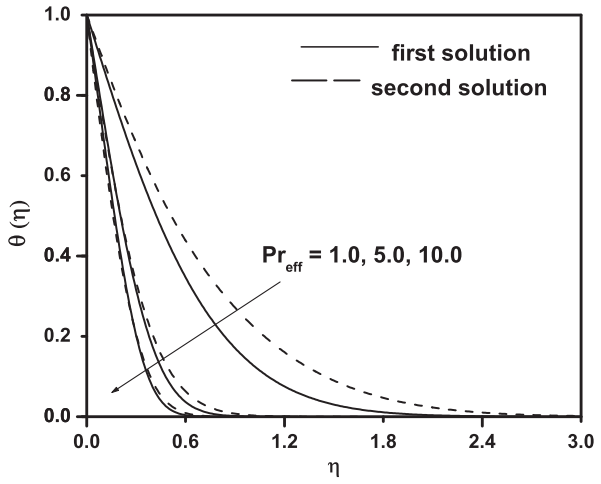

Figure 13 Variation of $\theta(\eta)$ for several values of Pr_{eff} when $s = 2.0$, $M = 1.0$, $A = -2.0$, $Le = 2.0$, $Nb = 0.5$, and $Nt = 0.5$.

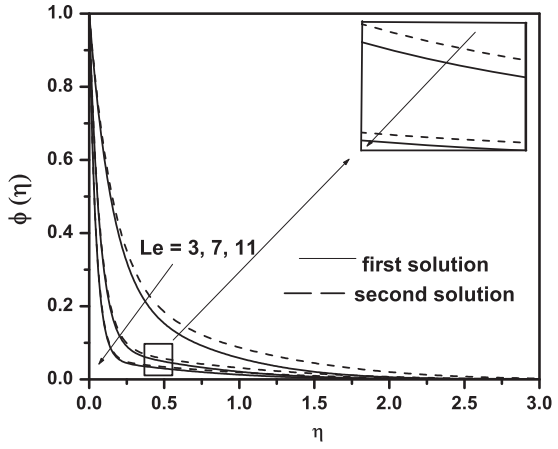

Figure 14 Variation of $\phi(\eta)$ for several values of Le when $s = 2.0$, $M = 1.0$, $A = -2.0$, $Nt = 0.5$, $Nb = 0.5$, and $Pr_{eff} = 0.71$.

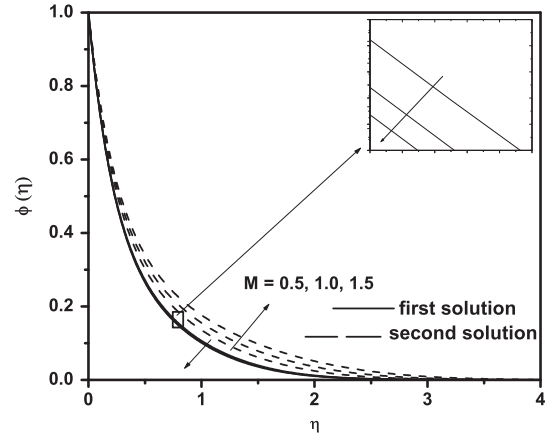

Figure 15 Variation of $\phi(\eta)$ for several values of M when $s = 2.0$, $A = -2.0$, $Le = 2.0$, $Nt = 0.5$, $Nb = 0.5$, and $Pr_{eff} = 0.71$.

ure reveals that as the wall mass suction parameter increases, the solution domain expands with the critical value of A moving to the left.

The numerical result reveals that dual solutions exist for certain values of the physical parameters. In order to ascertain which of the two solutions is expected to appear physically, the stability analysis of the dual solutions is required. Based on the stability analysis, only the first solution (upper branch) is stable and corresponds to the physically meaningful solution. On the other hand, the second solution (lower branch) is unstable and not physically meaningful. The relevant procedure can be found in studies reported by Merkin [32], Weidman et al. [33], Mahapatra et al. [34] and very recently by Rosca and Pop [35]. The novel result that emerges from the analysis is that, though two solutions exist mathematically, only the stable solution is physically meaningful and can be realized physically.

The variation of the heat transfer rate $-\theta'(0)$ and the concentration rate $-\phi'(0)$ with $A(< 0)$ for several values of the magnetic parameter M with fixed values of the other parameters is shown in Figs. 3 and 4 respectively. The dual nature of the solutions are also seen in these figures. From these figures, we can see that for the upper solution branch, due to an increment in value of M, both the heat transfer and the concentration rates increase. However for the lower solution branch, the opposite trend is observed.

Figs. 5–7 are drawn to analyze the influence of magnetic parameter (M), unsteadiness parameter (A) and wall mass suction parameter (s) on the horizontal velocity component $f'(\eta)$. Fig. 5 displays the variation of $f'(\eta)$ with η for several values of M. It is seen that horizontal velocity at a point increases with increase in M for the first solution and the opposite is true for the second solution. In fig. 6, the effect of unsteadiness parameter on the velocity profiles is shown for both the solution branches with fixed values of $s(= 2.1)$ and $M(= 0.2)$. The figure reveals that for both the solution branches, the velocity profiles are not monotonic. For the first solution branch, as the magnitude of the unsteadiness parameter (i.e, $|A|$) increases, $|f'(\eta)|$ decreases up to a point near the sheet but beyond this point opposite trend is observed. Fig. 7 illustrates the effect of the mass transfer parameter s on the horizontal velocity profile $f'(\eta)$ for two solution branches with $A = -1.0$ and $M = 0.2$. The figure reveals that the velocity penetration into the fluid becomes shorter with the increase of s for the upper solution branch and the velocity profiles penetrate deeper for a higher mass suction parameter.

The variation of $\theta(\eta)$ with η is shown in Fig. 8 for several values of M with fixed values of the other parameters. It is observed that temperature at a point decreases with increase in M for the first solution and the temperature increases with increase in M for the second solution. This is a consequence of the fact that the temperature field is influenced by the advection of the fluid velocity above the sheet. Fig. 9 shows the variation of temperature $\theta(\eta)$ with η for several values of the unsteadiness parameter $A(< 0)$. The figure reveals that the temperature at a point decreases as the magnitude of the unsteadiness parameter increases. This is due to the fact that the heat transfer rate increases with the increase in unsteadiness parameter which in turn reduces the temperature of the fluid. The temperature profiles for various mass suction parameter (s) are shown in Fig. 10. From the figure it is seen that the thermal boundary layer thickness decreases with increasing s. Physically this can be explained as follows; Due

to mass suction, the fluid is brought closer to the surface and consequently it prevents the vorticity diffusion. Also it is observed that, the thermal boundary layer thickness for the first solution is always thinner than that of the second solution.

The effects of thermophoresis parameter (Nt) and Brownian motion parameter (Nb) on the temperature profiles for selected values of parameters are shown in Figs. 11 and 12, respectively. As the parameters Nt and Nb increase, the temperature at a point increases. As a consequence, the thickness of the thermal boundary layer increases with the increase of Nt and Nb. The thermophoresis phenomenon describes the fact that small micron sized particles suspended in a non-isothermal gas will acquire a velocity in the direction of decreasing temperature. An increase in Nt results in an increase of the temperature difference between the sheet and the ambient fluid and consequently the thermal boundary layer thickness increases. Fig. 13 represents the influence of the effective Prandtl number (Pr_{eff}) on the dimensionless temperature profile. The temperature and the thermal boundary layer thickness reduce with Pr_{eff}. The physical reason is that, due to increase in Prandtl number (Pr), the thermal conductivity of the fluid reduces and consequently thermal boundary layer thickness decreases.

The effect of Lewis number (Le) on the dimensionless rescaled nanoparticle volume fraction $\phi(\eta)$ is shown in Fig. 14. It is observed that the concentration boundary layer thickness decreases with increasing Le. This is due to the decrease in mass diffusivity or the Brownian motion of the nanoparticle. Fig. 15 shows the variation of the dimensionless rescaled nanoparticle volume fraction $\phi(\eta)$ with magnetic parameter M in the concentration boundary layer. It is seen that the concentration boundary layer thickness decreases with magnetic parameter for the first solution and the opposite trend is observed for the second solution.

5. Concluding remark

The effects of magnetic, suction, thermal radiation, thermophoresis, Brownian motion and Lewis number parameters on the boundary layer flow and heat transfer of nanofluid over a shrinking sheet are investigated numerically using fourth order Runge–Kutta method with shooting technique. The effects of these parameters on dimensionless velocity, temperature, rescaled nanoparticle volume fraction, skin friction, rescaled Nusselt and Sherwood numbers can be summarized as follows:

1. The dual solutions are found to exist for the flow over a shrinking sheet.
2. The range of the existence of the solutions to the problem increases with increasing magnetic and suction parameters.
3. The dimensionless velocity increases with increasing magnetic and suction parameters for the first solution and decreases for the second solution.
4. The dimensionless temperature and the rescaled nanoparticle volume fraction both decrease with increasing M for the first solution and increase for the second solution.
5. The dimensionless temperature decreases with increasing values of unsteadiness, suction and effective Prandtl parameters but increases with increasing values of Nt and Nb.
6. The dimensionless rescaled nanoparticle volume fraction decreases with increasing Lewis number.
7. The magnitude of skin friction increases with increasing magnetic and suction parameters for the first solution and opppsite is true for the second solution.
8. The local Nusselt and Sherwood numbers increase with increase magnetic parameter for the first solution and decrease for the second solution.

Acknowledgements

We thank the reviewers for their helpful suggestions and comments, which enable to improve the presentation of the paper. One of the author S.K. Nandy is grateful to the University Grants Commission, New Delhi, India, for providing financial support under a Minor Research Project Grant No. F. PSW-002/13-14 to carry out the work.

References

[1] Sus Choi, Enhancing thermal conductivity of fluid with nanoparticles, developments and applications of non-Newtonian flow, ASME FED 231 (1995) 99–105.
[2] Sus Choi, Z.G. Zhang, W. Yu, F.E. Lockwood, E.A. Grulke, Anomalously thermal conductivity enhancement in nanotube suspensions, Appl. Phys. Lett. 79 (2001) 2252–2254.
[3] J. Buongiorno, Convective transport in nanofluids, ASME J. Heat Transfer 128 (2006) 240–250.
[4] D.A. Nield, A.V. Kuznetsov, The Cheng–Minkowycz problem for natural convective boundary layer flow in a porous medium saturated by a noanofluid, Int. J. Heat Mass Transfer 52 (2009) 5792–5795.
[5] A.V. Kuznetsov, D.A. Nield, Natural convective boundary layer flow of a nono fluid past a vertical plate, Int. J. Thermal Sci. 49 (2010) 243–247.
[6] D.A. Nield, A.V. Kuznetsov, The Cheng–Minkowycz problem for the double-diffusive natural convective boundary layer flow in a porous medium saturated by a nanofluid, Int J Heat Mass Transfer 54 (2011) 374–378.
[7] N. Bachok, A. Ishak, I. Pop, Boundary layer flow of nanofluids over a moving surface in a flowing fluid, Int. J. Thermal Sci. 49 (2010) 1663–1668.
[8] W.A. Khan, I. Pop, Boundary-layer flow of a nanofluid past a stretching sheet, Int. J. Heat Mass Transfer 53 (2010) 2477–2483.
[9] M.A.A. Hamad, Analytical solution of natural convection flow of a nanofluid over a linearly stretching sheet in the presence of magnetic field, Int. Commun. Heat Mass Transfer 38 (2011) 487–492.
[10] M.A.A. Hamad, M. Ferdows, Similarity solution of boundary layer stagnation-point flow towards a heated porous stretching sheet saturated with a nanofluid with heat absorption/generation and suction/blowing: a lie group analysis, Commun. Nonlinear Sci. Numer. Simul. 17 (2011) 132–140.
[11] N. Bachok, A. Ishak, I. Pop, Stagnation-point flow over a stretching/shrinking sheet in a nanofluid, Nanoscale Res. Lett. 6 (2011) 623–632.
[12] O.D. Makinde, A. Aziz, Boundary layer flow of a nanofluid past a stretching sheet with a convective boundary condition, Int. J. Thermal Sci. 50 (2011) 1326–1332.
[13] N. Bachok, A. Ishak, I. Pop, Flow and heat transfer characteristics on a moving plate in a nanofluid, Int. J. Heat Mass Transfer 55 (2012) 642–648.
[14] A. Alsaedi, M. Awais, T. Hayat, Effects of heat generation/absorption on stagnation-point flow of nanofluid over a surface with convective boundary conditions, Commun. Nonlinear Sci. Numer. Simul. 17 (2012) 4210–4223.

[15] W. Ibrahim, B. Sankar, M.M. Nandeppanavar, MHD stagnation point flow and heat transfer due to nanofluid towards a stretching sheet, Int. J. Heat Mass Transfer 56 (2013) 1–9.
[16] M. Miklavcic, C.Y. Wang, Viscous flow due to a shrinking sheet, Quart. Appl. Math. 64 (2006) 283–290.
[17] C.Y. Wang, Stagnation flow towards a shrinking sheet, Int. J. Nonlinear Mech. 43 (2008) 377–382.
[18] A. Ishak, Y.Y. Lok, I. Pop, Stagnation-point flow over a shrinking sheet in a micropolar fluid, Chem. Eng. Commun. 197 (2010) 1417–1427.
[19] K. Bhattacharyya, S. Mukhopadhyay, G.C. Layek, Slip effects on boundary layer stagnation-point flow and heat transfer towards a shrinking sheet, Int. J. Heat Mass Transfer 54 (2011) 308–313.
[20] K. Bhattacharyya, Dual solutions in boundary layer stagnation-point flow and mass transfer with chemical reaction past a stretching/shrinking sheet, Int. Commun. Heat Mass Transfer 38 (2011) 917–922.
[21] R.A. Van Gorder, K. Vajravelu, I. Pop, Hydromagnetic stagnation-point flow of a viscous fluid over a stretching/shrinking sheet, Meccanica 47 (2012) 31–50.
[22] Y.Y. Lok, A. Ishak, I. Pop, MHD stagnation-point flow towards a shrinking sheet, Int. J. Numer. Methods Heat Fluid Flow 21 (2011) 61–72.
[23] K. Das, Slip effects on MHD mixed convection stagnation point flow of a micropolar fluid towards a shrinking vertical sheet, Comput. Math. Appl. 63 (2012) 255–267.
[24] T. Fang, J. Zhang, S. Yao, Viscous flow over an unsteady shrinking sheet with mass transfer, Chin. Phys. Lett. 26 (2009) 014703.
[25] N. Bachok, A. Ishak, R. Nazar, I. Pop, Flow and heat transfer at a general three-dimensional stagnation point flow in a nanofluid, Physica B 405 (2010) 49144918.
[26] N. Bachok, A. Ishak, I. Pop, Unsteady boundary-layer flow and heat transfer of a nanofluid over a permeable stretching/shrinking sheet, Int. J. Heat Mass Transfer 55 (2012) 2101–2109.
[27] A.M. Rohni, S. Ahmad, A.I. Ismail, I. Pop, Flow and heat transfer over an unsteady shrinking sheet with suction in a nanofluid using Buongiorno's model, Int. Commun. Heat Mass Transfer 43 (2013) 75–80.
[28] J.A. Shercliff, A Textbook of Magnetohydrodynamics, Pergamon Press, Oxford, 1965.
[29] M.Q. Brewster, Thermal Radiative Transfer Properties, Wiley, New York, 1972.
[30] K. Vajravelu, K.V. Prasad, P.S. Datti, B.T. Raju, MHD flow and heat transfer of an Ostwald-de Waele fluid over an unsteady stretching surface, Ain Shams Eng. J. 5 (1) (2014) 157–167.
[31] I. Gladwell, D.K. Sayers, Computational Techniques for Ordinary Differential Equations, Academic Press, London, 1980.
[32] J.H. Merkin, On dual solutions occurring in mixed convection in a porous medium, J. Eng. Math. 20 (1986) 171–179.
[33] P.D. Weidman, D.G. Kubitschek, A.M.J. Davis, The effect of transpiration on self-similar boundary layer flow over moving surfaces, Int. J. Eng. Sci. 44 (2006) 730–737.
[34] T.R. Mahapatra, S.K. Nandy, K. Vajravelu, R.A. Van Gorder, Stability analysis of the dual solutions for stagnation-point flow over a non-linearly stretching surface, Meccanica 47 (2012) 1623–1632.
[35] A.V. Rosca, I. Pop, Flow and heat transfer of Powell–Eyring fluid over a shrinking surface in a parallel free stream, Int. J. Heat Mass Transfer 71 (2014) 321–327.